Published in final edited form as:

Adv Healthc Mater. 2019 April ; 8(8): e1801177. doi:10.1002/adhm.201801177.

Architectural Modification of Conformal PEG-Bottlebrush Coatings Minimizes Anti-PEG Antigenicity While Preserving Stealth Properties

Daniel Y. Joh[1,†], **Zackary Zimmers**[1,†], **Manav Avlani**[1,†], **Jacob T. Heggestad**[1], **Hakan B. Aydin**[1], **Nancy Ganson**[2], **Shourya Kumar**[1], **Cassio Fontes**[1], **Rohan K. Achar**[1], **Michael S. Hershfield**[2,3], **Angus M. Hucknall**[1,*], **Ashutosh Chilkoti**[1,*]

[1]Department of Biomedical Engineering, Pratt School of Engineering, Duke University, Durham NC 27708 USA.

[2]Department of Medicine, Division of Rheumatology, Duke University Medical Center, Durham, NC 27710 USA

[3]Department of Biochemistry, Duke University School of Medicine, Durham NC 27710 USA

Abstract

Poly(ethylene glycol) (PEG), a linear polymer known for its “stealth” properties, is commonly used to passivate the surface of biomedical implants and devices, and is conjugated to biologic drugs to improve their pharmacokinetics. However, its antigenicity is a growing concern. Here, we investigated the antigenicity of PEG when assembled in a poly(oligoethylene glycol) methacrylate (POEGMA) “bottlebrush” configuration on a planar surface. Using ethylene glycol (EG) repeat lengths of the POEGMA sidechains as a tunable parameter for optimization, we identified POEGMA brushes with sidechain lengths of two and three EG repeats as the optimal polymer architecture to minimize binding of anti-PEG antibodies (APAs), while retaining resistance to nonspecific binding by bovine serum albumin and cultured cells. We further investigated binding of backbone- versus endgroup-selective APAs to POEGMA brushes, and finally assessed the antigenicity of POEGMA coatings against APA-positive clinical plasma samples. We applied these results toward fabricating immunoassays on POEGMA surfaces with minimal reactivity toward APAs while retaining a low limit-of-detection for the analyte. Taken together, these results

*Correspondence to: Angus M. Hucknall (angus.hucknall@duke.edu) or Ashutosh Chilkoti (chilkoti@duke.edu).
†These authors contributed equally to this work

AUTHOR CONTRIBUTIONS

DJ, ZZ, and MA are co-lead authors, who participated in experimental design, data collection, data analysis, manuscript drafting, table/figure creation, and manuscript revision. JH, HA, SK, CF, and RA assisted with designing experiments, data collection, data analysis, and participated in manuscript drafting/revision. NG participated in experimental design and data collection in matters related clinical specimens. MH is a senior author involved in study design, oversight, and manuscript drafting/revision, particularly in matters related to clinical specimens. AH and AC co-directed the studies and were involved in drafting and revising the manuscript. All authors read and approved the final manuscript.

COMPETING INTERESTS

A.C. and A.H. are consultants to Immucor Inc., which has acquired the rights to the use of POEGMA for *in vitro* diagnostics from Sentilus Inc. (cofounded by A.C. and A.H.) and from Duke University. M.S.H. receives grant support from Leadiant BioSciences related to their FDA-approved product, Adagen (PEGylated bovine ADA). M.S.H. is also a co-inventor of Pegloticase (Kystexxa, PEGylated urate oxidase); M.S.H. and Duke University receive royalties on sales of Pegloticase from Horizon Pharma.

SUPPLEMENTARY INFORMATION

Supplementary Information accompanies this paper.

offer useful design concepts to reduce the antigenicity of polymer brush-based surface coatings used in applications involving human or animal matrices.

Keywords

polymer brush; POEGMA; anti-PEG; biofouling; antigenicity

INTRODUCTION

The immune responses that the widely-used polymer, poly(ethylene glycol) (PEG), can trigger is of growing concern [1]. Previously considered non-immunogenic [2, 3], linear PEG modification ("PEGylation") has become the most popular synthetic strategy to confer materials with "stealth" properties to eliminate protein adsorption and cell adhesion on surfaces, improve the biocompatibility of implanted biomaterials, and when conjugated to "biologics" —typically peptide and protein drugs and more recently aptamers— enhance their blood circulation and reduce their recognition by the immune system [4–6].

Products containing linear PEG constitute an estimated multi-billion-dollar market [7]. However, evidence supporting the existence and clinical relevance of anti-PEG immunity, namely in the form of anti-PEG antibodies (APAs), is mounting. PEGylated therapeutics are now known to induce APAs in both animals [8–10] and humans [11–19]. Further, APAs are known to be present in much of the general population, presumably from chronic exposure to PEG from consumer products, with approximately 37% showing moderate (≥ 100 ng/mL) and 8% showing high levels (≥ 500 ng/mL) of APAs [20, 21]. This potentially complicates the development of drugs, devices, or diagnostics modified with PEG (or PEG-derivatives), given the possibility of unwanted interference by APAs. In fact, clinical experience with PEGylated therapeutics has already indicated that APAs can not only cause increased clearance rates and loss of efficacy, but also can lead to serious anaphylactic or hypersensitivity reactions [11–19]. Notably, the issues posed by APAs has now been recognized by the Food and Drug Administration (FDA), which currently requests testing patients for APAs before treatment with experimental PEGylated compounds [22].

Several studies have proposed the use of alternative —non-PEG derived— stealth polymers such as polyzwitterions [23, 24], poly(2-ethyl 2-oxazoline) [25], and polyglycerol to circumvent this issue. However, transitioning to such polymers might offer an incomplete or temporary solution, for two reasons. First, antibodies (Abs) against other natural and synthetic polymers have been reported previously [26, 27], suggesting that other (non-PEG derived) stealth polymers might be capable of inducing an immune response after repeated administration over time. Second, both animal and human APAs were discovered to cross-react with other synthetic polymers [28]; this "polypharmacy" nature of polymer-reactive Abs likely adds further design constraints on candidate materials proposed as alternatives to PEG.

Instead, we and others believe that the large investments already made in PEGylation and its mainstream status underscore a pressing need to thoroughly investigate methods to tackle the emerging problem of 'PEG antigenicity' directly, without replacing PEG itself. Ideally,

this would be accomplished without the need for potentially aggressive interventions such as preemptive immunosuppression, pre-injection of large quantities of free PEG to saturate APAs or removing PEG altogether in select situations [18, 29, 30]. While these proposed strategies are intriguing, their downsides include potential additional risk to patients, reduction in therapeutic efficacy, suboptimal assay or device performance, and overall inconvenience.

Our work with poly(oligo(ethylene glycol) methyl ether methacrylate) (POEGMA) might offer an alternative, and less disruptive, solution. Specifically, over the past decade, we and others have explored POEGMA as an alternative to linear PEG for biomedical applications [5, 31–45]. POEGMA is a derivative of PEG with a "bottlebrush" architecture. POEGMA brushes show excellent "nonfouling" —protein- and cell-resistant— properties that make it a "stealth" polymer, like PEG. This is because POEGMA's three-dimensional hyperbranched structure presents a high density of oligoethylene glycol (EG) moieties [5, 46]. In a recent study, we discovered that drug-POEGMA conjugates having an average polymer sidechain length of nine EG units ("EG9") demonstrated significantly reduced anti-PEG antigenicity in patient plasma compared to two FDA-approved PEGylated protein drugs (Krystexxa® and Adagen®) [32, 47]. In the same study, we also observed that shortening the POEGMA side-chain length from EG9 to EG3 virtually eliminated the reactivity of the drug-POEGMA conjugates to APAs in patient plasma samples and did so without substantially compromising *in vivo* pharmacokinetics in animal models. We hence reasoned that replacing long, linear PEG structures (typically ≥ EG100) used in most PEGylated products with the shorter, hyperbranched structure of POEGMA (sidechains typically ≤ EG9) might offer a successful route towards mitigating antigenicity while simultaneously retaining acceptable stealth behavior. Realization of such a strategy would be a significant advancement, as it might potentially render POEGMA more efficacious than linear PEG for clinical applications. Further, the use of POEGMA —rather than transitioning to non-PEG derived polymers— may be logistically favorable given PEG's long history of use in humans and its pervasive role in commercial, research, and clinical settings [7].

These considerations motivated us to systematically investigate the length of EG sidechains on POEGMA as a design parameter that we could tune to mitigate POEGMA's reactivity toward APAs, while retaining its resistance to nonspecific binding. To do so, we chose to study these effects on POEGMA brushes grown as thin films from solid surfaces (Figure 1a), as opposed to solution studies of drug-polymer conjugates, for several reasons. First, planar polymer coatings are easy to synthesize and characterize with a variety of tools (e.g. X-ray spectroscopy, ellipsometry, contact angle goniometry). Second, this approach permits straightforward investigation of APA binding and nonspecific binding of proteins and cells directly on a POEGMA-grafted surface. Third, *in situ* growth of POEGMA from surfaces by surface-initiated atom transfer radical polymerization (SI-ATRP) is reliable and high-throughput. Fourth, this approach also enables investigation of how APAs might interfere in clinical devices and *in vitro* diagnostics (IVDs) [37–39, 42, 48–51].

Herein, we outline the synthesis and surface characterization of POEGMA coatings grown from glass substrates by SI-ATRP, encompassing a range of polymer brush sidechain lengths (EG1 to EG9). These POEGMA brush surfaces were subjected to a battery of screening tests

and subsequent down-selection processes aimed at identifying candidates that resist reactivity to APAs, protein adsorption —specifically, bovine serum albumin (BSA)— and adhesion of cultured cells. Next, we investigated how structural characteristics of bottlebrushes specifically contributed to mitigating binding by polymer endgroup-selective or backbone-selective APAs. Combined, these experiments revealed that POEGMA coatings with EG2 —and to a lesser extent, EG3— sidechains exhibit the most favorable performance in minimizing both APA recognition and nonspecific adsorption. As proof-of-concept, we directly validated these findings by measuring the binding of APAs to the POEGMA brush surfaces from plasma samples from patients previously treated with a PEGylated drug (Krystexxa®) and found to have induced or pre-existing APAs [12]. Given the relevance of POEGMA surfaces to immunodiagnostic applications, we then examined the response of protein microarray immunoassays fabricated onto POEGMA surfaces with different EG side-chain lengths that were run in the presence of APAs.

Our results are potentially valuable for the implementation of next-generation, PEG-derived polymer brush coatings designed for products that biologically interface with human (or animal) matrices that might contain APAs. More broadly, this work highlights the potential advantages of using surface-based analyses for efficient screening and guided optimization of polymer architectures in biomedically-relevant contexts.

RESULTS & DISCUSSION

Growth and characterization of POEGMA brushes with varying sidechain lengths

Our strategy to coat planar surfaces with POEGMA bottlebrushes by SI-ATRP is illustrated in Figure 1a [37, 39]. Glass surfaces were first functionalized with a brominated ATRP initiator, followed by SI-ATRP of oligoethylene glycol methacrylate monomers via activators regenerated by electron transfer (ARGET) for *in situ* synthesis of the POEGMA brush surfaces on glass; this synthesis strategy has been previously shown to result in uniform POEGMA coatings with controllable film thicknesses under relatively mild experimental conditions [37, 52–54]. To systematically tune the sidechain length of POEGMA bottlebrushes, SI-ATRP was carried out using different commercially-available PEG methacrylate monomers with varying number of EG repeat units. The properties of each monomer are listed in Figure 1b, which on average ranged from 1 to 9 EG repeats. The specific SI-ATRP reaction conditions used to synthesize each of these polymer brush surfaces can be found in Table S1. The side chain of each monomer was terminated by a methoxy (-OMe) endgroup, except the ~360 Da monomer which had a hydroxy (-OH) endgroup. Hereafter, each surface will be referenced by both their average EG repeat length and endgroup (i.e. EG2-OMe).

Following growth of the POEGMA overlayers by SI-ATRP, characterization of the POEGMA bottlebrushes was performed in three ways. First, the thickness of the POEGMA overlayers was measured by reflective mode spectroscopic ellipsometry. Based on our earlier work, we sought to synthesize polymer coatings with thicknesses greater than ~10 nm, as we observed that this was the minimum thickness required to achieve consistent nonfouling behavior [41, 45]. As indicated in Figure 1c, our experimental thicknesses were consistently ~25 nm or greater, and thus were well above this threshold. Second, we assessed the

wettability of each surface by contact angle goniometry (Figure 1d). We observed a progressive increase in wettability of each polymer surface, as seen by decreasing contact angles, with increasing number of EG repeats. There was a statistically significant difference between groups, as determined by one-way ANOVA ($F(6, 37) = 136.0$, $p < 0.0001$). Bars marked with a different letter indicates significant differences (Tukey post hoc test, $p \leq 0.05$). This result is consistent with the expectation that monomers with longer EG repeats would present greater densities of hydrophilic oligo(ethylene glycol) functional groups at the solid/water interface.

Third, the molecular composition of the films was investigated by X-ray photoelectron spectroscopy (XPS) (Figure S1). In all cases, the survey spectra of the polymer-coated samples demonstrated the absence of Si peaks (from the underlying glass after polymerization (Figures S1a–g). This observation is consistent with the film thicknesses being greater than the sampling depth of the XPS—typically ~10 nm for Al Kα radiation [55]—resulting in the vast majority of detected photoelectrons originating from the polymer overlayer. The observed carbon and oxygen atomic concentrations measured from the survey spectra for each POEGMA surface agreed with those expected from their stoichiometry (Figure S1h). Furthermore, analysis of the high-resolution O1s and C1s photoemission spectra in Figures S1a–g indicated the presence of a sole oxygen species that is singly-bonded to an aliphatic carbon (532.8 eV), and three distinct carbon moieties: CH_x (284.5 eV), COR (286.7 eV), and COOR (289.1 eV). Deconvolution of the C1s envelopes to each of these carbon species also showed agreement between experimental and predicted values (Figure S1h).

Combined, these experiments confirmed that our fabrication methods produced POEGMA coatings with adequate thickness, predictable interfacial hydration, and appropriate chemical composition. Having synthesized and characterized the desired polymer surfaces, we next screened POEGMA surfaces for their: (1) reactivity to APAs and (2) nonspecific binding of BSA and cultured cells, so as to identify coatings that minimize both attributes.

Preliminary screening reveals EG2-OMe and EG3-OMe bottlebrushes minimize APA reactivity and nonspecific binding by BSA and cultured fibroblasts

We first assessed the reactivity of the polymer coatings toward a rabbit-derived polyclonal APA (“pAPA1”) using a surface fluoroimmunoassay, as illustrated in Figure 2a. Each polymer coating was first incubated with 2 μg/mL pAPA1 spiked into calf serum (to simulate circulating APAs), which was applied directly to the surface, and then rinsed with a standard PEG-free wash buffer (0.5% 3-[(3-Cholamidopropyl)-dimethylammonio]-1-propane sulfonate (CHAPS) detergent in phosphate-buffered saline (PBS)) to remove loosely bound pAPA1. Surfaces were then labeled with a Cy-5-anti(α)-rabbit detection Ab (dAb), and fluorescence intensities were quantified by a tabletop fluorescence scanner to quantify the Cy5 signal from the surface-bound dAb, whose intensities are expected to scale with the surface concentration of APA bound to the polymer surface (Figure S2). Vehicle controls (serum only) established baseline fluorescence values, and negative controls comprised of control rabbit IgG in serum (in lieu of rabbit-derived pAPA1) showed that adventitious binding of rabbit IgG did not noticeably contribute to nonspecific background

noise under these experimental conditions (Figure 2b and Figure 2c). This was true even for bare glass; detergent-containing PBS wash buffer was able to remove loosely bound rabbit IgG from the surface (but PBS alone was not, see Figure S3). We observed a large increase in Cy5 fluorescence for EG5-OMe, EG6-OH, and EG9-OMe surfaces, but near-baseline response for EG1-OMe, EG2-OMe, and EG3-OMe surfaces (Figures 2b–c). One-way ANOVA indicated that there was a statistically significant difference between pAPA1-treated groups ($F(6, 33) = 50.05$, $p < 0.0001$). Bars marked with different letters in Figure 2c indicate significant differences within the pAPA1-treated groups (Tukey post hoc test, $p \leq 0.05$) indicating that reactivity to pAPA1 is significantly lower for POEGMA brush surfaces with EG3 and smaller sidechains.

We observed a decreasing trend in fluorescence between the smaller sidechain moieties, namely EG3-OMe (276 a.u.) > EG2-OMe (157 a.u.) > EG1-OMe (63 a.u.); while notable, the difference between these groups was not statistically significant by one-way ANOVA analysis. Additionally, while the hydroxy-terminated EG6-OH surface was clearly reactive to pAPA1, we observed a lower response when compared to that of methoxy-terminated EG5-OMe and EG9-OMe. This finding is consistent with previous studies showing that hydroxy-terminated PEG is less antigenic than methoxy-terminated PEG against APAs derived from methoxy-PEG immunogens [56–58]. This is indeed the case for pAPA1, which is a polyclonal Ab (pAb) generated by immunization with methoxy-terminated linear PEG with 24 EG repeats that shows considerable reactivity to PEG end-groups (see Methods).

Next, we compared the stealth functionality of the POEGMA brushes by evaluating their ability to prevent nonspecific binding of proteins and cells on these surfaces (Figure 3). Protein adsorption was assessed using BSA, a protein well-known for its tendency to adsorb to surfaces [59]. Surfaces were incubated with Cy5-labeled BSA (Cy5-BSA), rinsed with 0.1% Tween20 in PBS to remove any loosely-bound proteins, and then imaged with a fluorescence scanner to detect residual Cy5-BSA avidly bound to the surface (Figure 3a). The raw fluorescence intensity for each surface is shown in Figure 3b and are quantified in Figure 3c as mean ± 95% confidence interval (CI). There was a statistically significant difference between Cy5-BSA-treated groups in Figure 3c, as determined by one-way ANOVA ($F(5, 31) = 390.2$, $p < 0.0001$). Bars marked with different letters indicate significant differences (Tukey post hoc test, $p \leq 0.05$). The uncoated glass surface showed the highest level of nonspecific adsorption of Cy5-BSA (Figures 3b–c). Next, while EG1-OMe coatings reduced overall binding to some extent, we observed considerable fluorescence response from residually-bound Cy5-BSA on the EG1-OMe brush. In contrast, POEGMA brushes with average sidechain lengths of EG2 or greater showed considerably lower nonspecific BSA adsorption.

A similar trend was observed when investigating the adhesion of cultured fibroblast cells to the surface (Figure 3d). Here, each surface was incubated with a solution of complete growth medium containing immortalized fibroblast cells expressing GFP (3T3-GFP) for 24 h, followed by rinsing and medium exchange, and epifluorescent imaging of GFP was then carried out to identify adherent cells. The fluorescence intensity was quantified by calculating percentage of pixels in the field of view showing positive signal in the GFP channel to represent surface coverage by cells (‘% FOV). Results are plotted as mean of the

%FOV ± 95% CI for at least 6 images per group. There was a statistically significant difference between groups, as determined by one-way ANOVA $F(6, 36) = 122.2$, $p < 0.0001$). Bars marked with different letters indicate significantly different groups (Tukey post hoc test, $p \leq 0.05$). Consistent with our BSA adsorption experiments, considerable adhesion of 3T3-GFP cells was observed for both uncoated and EG1-OMe surfaces but was virtually eliminated on POEGMA brushes with EG2 or longer sidechains (Figures 3e–f). Taken together, these initial downselection experiments indicated that EG2-OMe and EG3-OMe POEGMA surfaces were the most viable candidates for meeting the established constraints of minimizing APA reactivity, BSA adsorption, and cell adhesion.

Building upon these initial downselection experiments, we next sought to directly compare the binding of pAPA1 to POEGMA brushes versus that of linear PEG. Specifically, we used inkjet-printing [37] to immobilize microspots of linear PEG-protein conjugates (PEG20K-BSA) known to be APA-reactive onto EG2-OMe, EG3-OMe and EG5-OMe POEGMA brushes (schema shown in Figure 4a). The surfaces were exposed to a dilution series of rabbit-derived pAPA1 in serum and then labeled with Cy5-donkey-α-rabbit dAbs and subsequently imaged on a fluorescent scanner. On EG2-OMe surfaces, we observed highly asymmetric APA reactivity in areas functionalized by PEG20K-BSA. EG2-OMe POEGMA background shows minimal signal, while an intense and spatially well-defined fluorescence response is observed in the circular feature defined by the printed PEG20K-BSA microspot (Figure 4b). In quantitating the Cy5 signal in the surrounding EG2-OMe polymer brush to assess APA binding, baseline values of fluorescence were observed across all pAPA1 concentrations up to 2 μg/mL (open circles, Figure 4c). In contrast, the microspots of PEG20K-BSA showed a dose-dependent Cy5 signal that scaled with increasing concentrations of pAPA1 analyte (black squares, Figure 4c). Using the concentration curve derived from the PEG20K-BSA Ag spots, we calculated an LOD ("LOD_{Ag}") of 1.4 ng/mL for pAPA1 fabricated on EG2-OMe POEGMA surfaces. An LOD for the polymer brush background ("LOD_{bkg}") could not be calculated in this case given the lack of dose-dependent behavior for the EG2-OMe POEGMA background, consistent with the fact that pAPA1 lacks affinity for EG2-OMe POEGMA.

Similar behavior was observed for EG3-OMe surfaces (Figure 4d–e), and a similar LOD_{Ag} of 0.86 ng/mL was determined for pAPA1 binding to PEG20K-BSA. The Cy5 signal from the EG3-OMe POEGMA brush background remained at baseline values for the majority of pAPA1 concentrations (Figure 4e). We did, however, note a gradual rise in background values at much higher pAPA1 concentrations; this behavior is consistent with the low level of binding of pAPA1 to EG3-OMe POEGMA observed in Figure 2b. This allowed us to estimate a LOD_{bkg} of 249.5 ng/mL. In contrast, we observed that the sharply asymmetric reactivity to pAPA1 is lost for EG5-OMe POEGMA surfaces (Figure 4f–g), as evidenced by the highly robust response to pAPA1 in both the Ag (BSA-PEG20K) spots and the POEGMA brush background. The calculated LOD_{Ag} and LOD_{bkg} for these surfaces were similar at 1.4 and 1.5 ng/mL, respectively (Figure 4g).

EG2-OMe and EG3-OMe bottlebrush reactivity toward endgroup-selective versus backbone-selective APAs

We next sought to better understand how APAs targeting different structural features of PEG (methoxy endgroup vs. backbone) might uniquely interact —if at all— with EG2-OME and EG3-OMe POEGMA brush surfaces. We began our investigation by measuring the surface reactivity of EG2-OMe, EG3-OMe, and EG5-OMe surfaces with pAPA1 versus another rabbit-derived pAb —pAPA2— that is selective for the PEG backbone rather than the mPEG endgroup (as is the case for pAPA1; see Methods) (Figure 5a). Each surface was incubated with pAPA1- or pAPA2-spiked serum at 2 μg/mL and then labeled with a Cy5-dAb (Figure 5b). This APA concentration was chosen based on previous results that individuals in the general population documented to have "high levels" of APA (≥ 500 ng/mL) have values reaching up to 2 – 6 μg/mL [20].

The raw fluorescence images for binding of pAPA1 and pAPA2 are shown in Figure S3a. The quantified data, shown in Figure 5c for pAPA1 and Figure 5d for pAPA2, indicate a statistically significant difference between groups for each polyclonal APA as determined by one-way ANOVA ($F(2, 24) = 268.1$, $p < 0.0001$ for pAPA1, and $F(2, 24) = 62.3$, $p < 0.0001$ for pAPA2). As observed previously, EG2-OMe and EG3-OMe were resistant to pAPA1 binding, compared to EG5-OMe (Figure S5a (top row) and Figure 5c). However, after exposure to 2 μg/mL pAPA2, we observed considerable pAPA2 binding to both EG3-OMe and EG5-OMe surfaces, whereas EG2-OMe surfaces remained resistant (Figure S5a (bottom row) and Figure 5d). These results suggest that EG3-OMe POEGMA brushes might be selectively resistant to endgroup-reactive APAs but not backbone-reactive APAs, whereas EG2-OMe may be resistant to both.

To explore this finding further, we then exposed the same surfaces to endgroup- vs. backbone-selective monoclonal APAs (e-mAPA vs. b-mAPA, respectively) under similar conditions as in the previous experiment. We observed robust binding of e-mAPA by the EG5-OMe POEGMA brush, but not by EG2-OMe or EG3-OMe brush at 2 μg/mL (similar to pAPA1) (Figure S5b, top row). In contrast, b-mAPA was found to react with both EG3-OMe and EG5-OMe surfaces but not with EG2-OMe (Figure S5b, bottom row). The quantified fluorescence intensity of the images and are shown in Figure 5e for e-mAPA and in Figure 5f for b-mAPA. The data show a statistically significant difference between groups for each APA, as determined by one-way ANOVA ($F (2, 24) = 319.5$, $p < 0.0001$ for e-mAPA, and $F (2, 24) = 222.0$, $p < 0.0001$ for b-mAPA). As shown in Figures 5e–f, the binding behavior of these monoclonal APAs effectively recapitulated that of pAPA1 and pAPA2 (Figures 5c–d). In addition to these studies using monoclonal APAs having IgG subtype, we also performed similar experiments using backbone-selective IgM subtype APAs (Figure S6), and as expected their behavior overall paralleled that of b-mAPA and pAPA2 (Figure 5f).

From these data, we deduce the following: (1) Sufficiently shortening the sidechains of POEGMA bottlebrushes to EG3 and shorter eliminates reactivity to endgroup-selective APA clones. Notably, this is achieved without needing to replace the more commonly-used (and stable) methoxy termini with a more reactive hydroxy endgroup. (2) Avoiding reactivity to backbone-specific APAs, however, requires a further reduction in sidechain length from EG3

to EG2; this effect is likely related to reducing the epitope length to shorter than the previously reported minimum of 3 EG units required for APA recognition [60].

Assessing the antigenicity of EG2-OMe, EG3-OMe, and EG5-OMe bottlebrushes toward APA-positive patient plasma

We next investigated the reactivity of EG2-OMe, EG3-OMe, and EG5-OMe POEGMA brush coatings against plasma samples of patients who were previously treated with a PEGylated drug, Krystexxa®. We tested plasma samples from 4 different patients from this cohort (samples P1-P4) and one patient known to be APA-negative (sample N1) using protocols described previously (see Methods) [11, 12, 14]. We performed an indirect ELISA on these patient plasma samples to quantify the level of IgG binding to Adagen (PEGylated adenosine deaminase). Sample N1 exhibited baseline values compared to pooled APA-negative reference standards, while P1-P4 tested positive for reactivity toward Adagen (rank order P4 > P3 ≈ P2 > P1), as expected (Table S2 and Figure 6). Next, these samples were applied to EG2-OMe, EG3-OMe, and EG5-OMe and assessed for surface reactivity using a Cy5-goat-α-human IgG Ab, using a procedure similar to the approach shown in Figure 2. As expected, the highest level of binding in this group is observed from EG5-OMe surfaces, as seen by the highest fluorescence intensities, which scaled according to the rank-ordering of Adagen reactivity by ELISA (Figure 6). This was followed by EG3-OMe, which behaved in a similar manner but exhibited noticeably more resistance to APA binding than EG5-OMe. Finally, EG2-OMe surfaces showed the lowest levels of reactivity within the group toward APA-positive samples. Interestingly, sample P2 elicited a modest increase in fluorescence on EG2-OMe compared to other positive samples tested on this surface (reaching similar intensity levels as EG3-OMe, but much less than EG5-OMe). By and large, results from these experiments obtained from human plasma generally parallel our findings observed above in simulated specimens, wherein antigenicity of PEG-derived bottlebrushes is correlated with EG sidechain length.

Application toward indirect sandwich immunoassay IVDs fabricated on POEGMA

Finally, we sought to investigate settings other than drug delivery [32], under which the lack of PEG antigenicity of the EG2 and EG3 POEGMA coatings might have practical or translational relevance. In particular, our group has been interested in the use of conformal POEGMA films as novel “zero-background” passivating surfaces to enhance the overall performance of next-generation immunoassays [5, 37–39]. Immunoassays on POEGMA have several advantages over traditional formats, namely the enzyme linked immunosorbent assay (ELISA). Biological reagents can be directly printed onto the polymer brush surface without the need for covalent coupling, and the brush stabilizes printed reagents so that they remain active for prolonged periods without refrigeration. Further, POEGMA films minimize nonspecific binding of cells and proteins on the assay surface; this permits high signal-to-noise ratios in the assay, even in complex biological samples (e.g. whole blood) without needing to perform sample preprocessing or additional surface blocking steps [37]. Although our group has also recently studied the use of zwitterionic (i.e. non-PEG derived) polymer brush films as APA-resistant substrates for immunoassay fabrication [61], here we sought to investigate whether a similar effect could be achieved on PEG-derived bottlebrush surfaces.

We thus investigated the indirect sandwich immunoassay (ISIA), a popular serology assay format, in which host-derived anti-antigen (Ag) Abs in circulation first bind to pathogen Ags immobilized on a POEGMA-coated assay surface. These bound Ab-Ag complexes are subsequently labeled with dAbs that bind host-derived Abs. Recent reports estimating APA levels in the general population [20, 21] led us to consider whether so-called 'moderate' levels of APA (≥100 ng/mL) might be problematic for the performance of serology ISIAs fabricated on nonfouling POEGMA coatings. In this case, host APAs in circulation that recognize and bind to PEG epitopes across the polymer surface would subsequently get labeled (along with the desired pathogen-specific host Abs), thereby introducing background noise and impairing the sensitivity of the assay.

As proof-of-concept, we simulated these ISIA conditions on POEGMA for the detection of circulating anti-HIV p24 Abs (Figure 7a). ISIAs were fabricated by noncovalently printing HIV p24 Ag as microspots onto POEGMA-coated surfaces [37]. The printed surfaces were then incubated with a dilution series of analyte —rabbit- α-p24 pAbs— spiked into undiluted serum, either with or without 100 ng/mL of rabbit-derived pAPA1 added as an interferent; hence, the Abs were species-matched to recapitulate host-derived APA interference. This was followed by rinsing and then labeling with Cy5-donkey-α-rabbit dAbs (the microspot images are shown in Figure S7). The performance of ISIAs fabricated on EG1-OMe, EG2-OMe, and EG3-OMe surfaces were virtually unaffected by the presence of pAPA1 interference as seen by the overlap of concentration curves against anti-p24 pAb analyte and overall similarities in their calculated limits-of-detection (LODs) (Figures 7b–d). However, for surfaces with longer EG sidechains (EG5-OMe and EG6-OH) that showed considerable APA reactivity in earlier screening experiments (Figure 2), we similarly observed significant interference by pAPA1 and loss of assay sensitivity due to marked elevation in background noise from surface-bound APAs (Figures 7e–f). We calculated that the presence of pAPA1 led to a 40-fold increase in LOD for assays fabricated on EG6-OH polymer brush surfaces. Further, the introduction of pAPA1 to EG5-OMe based assays produced so much interference that an LOD was not calculated in this case.

DISCUSSION

We synthesized conformal POEGMA brush coatings by solution-based batch processing of glass substrates (via SI-ATRP), and we systematically investigated the number EG repeats as a design parameter to minimize: (1) APA antigenicity and (2) BSA adsorption and fibroblast adhesion. These studies identified EG2-OMe —and to a lesser extent, EG3-OMe— POEGMA brush surfaces as having the optimal architecture to minimize both attributes.

In our previous work, we observed that drug-POEGMA conjugates with EG3-OMe sidechains virtually eliminated PEG antigenicity when tested against patient plasma samples and assayed in conventional ELISA experiments involving Adagen® and Krystexxa® [32]. As with those studies, the present work on planar surface coatings revealed that EG3-OMe POEGMA brushes show minimal recognition by endgroup-selective APAs; however, we also report two new interesting observations. First, we show that EG3-OMe bottlebrush surfaces exhibit some, albeit low level of binding to backbone-selective APAs (Figure 5). The tendency for EG3-OMe bottlebrushes to bind backbone-selective but not endgroup-

selective APAs is somewhat counterintuitive, as methoxy endgroups in POEGMA sidechains are more ‘exposed’ than backbones. It is possible that bottlebrushes with longer EG repeats might have greater sidechain mobility to accommodate binding of endgroup-selective APAs to 3 terminal EG units (the minimum required for antigenicity [60]) in a sterically favorable manner. Conversely, we speculate that the reduced mobility of shorter sidechains in EG3-OMe bottlebrushes, combined with the requirement of binding to 3 EGs at sidechain termini in the appropriate orientation, might render binding of endgroup-selective APAs toward EG3-OMe brushes unfavorable, yet more studies are necessary to elucidate this phenomenon. Second, consistent with the first observation, we show that surface-grown EG3-OMe exhibits some antigenicity toward APAs in human plasma, which was not observed in our previous work [32]. We attribute these differences, at least in part, to several factors. Patient plasma is expected to contain populations of both endgroup- and backbone-selective APAs, with larger titers of the former based on its greater immunogenicity [56, 57, 62]. Hence, based on our current data, we speculate that the EG3-OMe drug conjugates in our earlier work avoided recognition by mostly endgroup-selective clones. However, measurement of the remaining backbone-selective clones that may have successfully bound to EG3-OMe drug conjugates likely fell below the detection limit of the ELISA used in that work. In contrast, using a more sensitive readout in the present work (the surface fluoroimmunoassay on the POEGMA brush) [37] made it possible to detect low levels of backbone-selective APA binding on EG3-OMe surfaces. From a practical standpoint, most current PEGylated therapeutics (immunogens) are mPEG-modified, which are known to stimulate a fairly robust population of endgroup-directed clones when an immune response is elicited [57]. This biological tendency, combined with (i) our prior observations with drug-POEGMA conjugates and (ii) the noticeable reduction in antigenicity in both simulated and human specimens by EG3-OMe shown herein, suggest that drugs conjugated to EG3-OMe brushes might be sufficiently evasive toward APAs in clinical practice.

In addition to studies by our group and others on protein-polymer conjugates supporting the claim that the hyperbranched architecture of POEGMA leads to a reduction in antigenicity compared to long-chain linear PEG [31–33], similar comparisons were also made in a recent investigation on planar surface-grafted polymers by Zhang *et al* [63]. The authors fabricated surface plasmon resonance sensors (SPRSs) functionalized with linear PEG versus POEGMA overlayers and compared their response to APAs. Consistent with our previous work [32], long-chain linear 5 KDa PEG (“PEG5K”) grafted to gold surfaces on SPRSs were more reactive to APAs than EG9-OMe bottlebrushes grown by SI-ATRP. Next, although replacing linear PEG5K with linear EG4 self-assembled monolayers (SAMs) reduced APA binding below the detection limit of their measurements, the linear EG4 SAM surfaces noticeably suffered from nonspecific binding of serum proteins. While the extent of nonfouling behavior exhibited by EG3- to EG6-SAMs is debated in the literature [64–66], results from the present study show that assembling even shorter (EG2 to EG3) PEG moieties into a hyperbranched bottlebrush on a surface resists APA binding (EG2 more effectively than EG3) and also effectively minimizes adsorption by BSA and fibroblast cells. Additionally, PEG5K-coated SPRSs used in an ISIA format for APA sensing (chosen over EG9-OMe polymer brush SPRSs given greater APA reactivity) showed LODs of 10 to 50 ng/mL against APAs spiked into saline buffer. In contrast, the POEGMA-based anti-PEG

assays described in the present work (Figure 4)—whether measuring the local response of BSA-PEG20K microspots printed on EG2-OMe/EG3-OMe surfaces (Figures 4c, e), or the total response of an entire EG5-OMe surface (Figure 4g)—exhibited a far lower LOD of ~1–2 ng/mL in detecting APAs in undiluted serum. Hence, surface fluorescence measurements on PEG-derived bottlebrush coatings as described herein may offer a straightforward and highly sensitive assay for APAs in clinical samples compared to SPR based assays and ELISA.

Although our focus in the present study is on surface-based screening of APAs and biofouling with application in immunodiagnostics, we recognize the importance of PEGylation in drug delivery and hence we qualitatively assessed how results from surface screens might translate to drug-POEGMA conjugates [32]. Our results suggest that surface-based screening for APA binding agrees with results obtained for soluble drug-POEGMA conjugates, and that anti-biofouling behavior on POEGMA brush surfaces might be a good proxy for favorable —long circulation— pharmacokinetics of POEGMA conjugates in solution.

We are mindful of the concerns surrounding anti-PEG immunity, and that its relevance to human patients are still in the infant stage [67, 68]. There is still debate as to why some patients mount a robust immune response to PEG while others do not, and clarification is needed as to why administering PEG-modified products only sometimes generates clinically-observable outcomes. While thus far clinically-observable reaction to PEGylated drugs (e.g. accelerated clearance or hypersensitivity) have mostly been limited to patients with high titers of APAs [14, 19, 69], there is evidence that even low-to-medium titers of anti-drug Abs against other agents have been reported to alter their pharmacological behavior *in vivo* [70], justifying more thorough investigation of the APA response in patients. We also emphasize that results from the present study must be interpreted with caution since they focused on the antigenicity of POEGMA against APAs and did not investigate its immunogenicity. More studies are necessary to determine whether exposure to POEGMA conjugates can generate a robust, POEGMA-specific humoral response.

Nevertheless, given increasing reported cases of PEG-related complications in clinical settings, the prevalence of APAs in the general population, and the already considerable (and growing) investment into PEG-modified products, the results of our study, we believe, are broadly relevant to diagnostics and implants that might benefit from using POEGMA bottlebrushes as next-generation bioinert coatings and as a potential alternative to linear PEG for drug conjugation.

METHODS

Surface-initiated atom transfer radical polymerization.

(A) Surface functionalization with APTES and installation of bromide initiator: Unless otherwise stated, steps were performed under ambient conditions. Glass slides (Nexterion Glass B, Schott AG, Mainz, Germany) were immersed in a 10% solution of 3-aminopropyltriethoxysilane (APTES) (Gelest, Inc.; Morrisville, PA) in ethanol overnight, and subsequently rinsed with fresh ethanol and then with deionized water. Chips were spun

dry at 150 rcf for 5 min and then cured in an oven at 110°C for 2 h. Next, the chips were cooled to room temperature then placed in a dichloromethane solution containing 1% α-bromoisobutyryl bromide (BIB) and 1% triethylamine (TEA) (Sigma Aldrich; St. Louis, MO) for 45 min, followed by rinsing in fresh dichloromethane, then ethanol, and then in deionized water. The chips were spun dry 150 rcf for 5 min and then stored under ambient conditions. (*B) Preparation of polymerization solution*: Degassed polymerization solutions were prepared as described in Table S1 and then transferred into an inert (Ar environment) glovebox. (*C) Surface-initiated atom-transfer radical polymerization*: In an Ar environment, sodium ascorbate (Sigma Aldrich; St. Louis, MO) was added to the polymerization solution described above and gently stirred for 1 min (specific amount of sodium ascorbate for each monomer is listed in Table S1), at which point the solution changed color from blue to violet. Initiator-functionalized glass slides were then placed in this solution for polymerization (without stirring). After allowing polymerization to proceed for the desired time points (Table S1), slides were rinsed three times with deionized water, then centrifuged at 150 rcf for 6 min and allowed to dry under ambient conditions. The thickness of polymer brushes was determined by reflective-mode ellipsometry, as described below.

Reflective Mode Ellipsometry.

The thickness of thin films was measured using an M-88 spectroscopic ellipsometer (J.A. Woollam Co) at angles of 65, 70, and 75 degrees at wavelengths of 400 to 800 nm. Polymer film thicknesses were then determined using a Cauchy layer algorithm. For all ellipsometric measurements, we chose the thickness for which the mean standard error between the predicted response from the model and the experimental response from the sample reached a global minimum. Only those data that yielded good fitting results (mean square error ≤ 0.9) were used to determine film thicknesses.

X-ray Photoelectron Spectroscopy.

All XPS experiments were performed on an AXIS Ultra photoelectron spectrometer (Kratos Analytical, NY) operating at 15 kV and 10 mA using monochromatic Al Kα1 x-rays. The x-ray spot size was 400 μm (full-width at half maximum). Survey scans and high-resolution core-level spectra were recorded with the following pass energy, energy step, dwell time, and number of sweeps: survey spectra - 160 eV, 1 eV, 200 msec, and 10 sweeps; high-resolution core-level spectra - 20 eV, 0.1 eV, 269.7 msec, and 20 sweeps. The operating pressure of the instrument was ~1×10^{-8} torr. The spectral data were analyzed using CasaXPS software [71].

Surface fluoroimmunoassays for anti-PEG reactivity in simulated samples.

The commercial APAs used in these studies were the following: pAPA1 – polyclonal rabbit-anti-PEG Abs (ThermoFisher PA5–32247); pAPA2 - polyclonal rabbit-anti-PEG (Life Diagnostics PEGPAB-01); e-mAPA – monoclonal mouse anti-PEG IgG Ab (Life Diagnostics 5D6–3); b-mAPA – monoclonal mouse anti-PEG IgG Ab (Life Diagnostics 1D9–6); and a monoclonal rabbit-anti-PEG IgM Ab (abcam AB133471). Surfaces were first exposed to a 2 μg/mL solution of APA-spiked calf serum and incubated for 1 h, and then washed 3 times with wash buffer (0.5% CHAPS in PBS). Next, the surfaces were exposed to a 2 μg/mL solution of Cy5 labeled dAb in PBS for 30 mins (donkey-anti-rabbit dAb or goat-

anti-mouse dAb, R & D Systems, Inc.). Surfaces were then rinsed again to remove any loosely-bound proteins with 0.1% CHAPS in PBS, centrifuged at 4800 rpm for 15 s to wick away excess liquid, then allowed to dry under ambient conditions. Fluorescence imaging of all samples was performed using an Axon Genepix 4400 tabletop scanner (Molecular Devices, LLC; Sunnyvale, CA) under identical imaging conditions with an exciting wavelength of 635 nm; fluorescence intensity analysis was performed using ImageJ Fiji [72].

BSA Adsorption.

Surfaces were exposed to a 1 mg/mL solution of Cy5-BSA (ThermoFisher) in 1X PBS for 2 h. Substrate were then rinsed with a PBS solution containing 0.1% (v/v) Tween20 to remove any loosely-bound Cy5-BSA, centrifuged at 4800 rpm for 15 s to wick away excess liquid, then allowed to dry under ambient conditions. Fluorescence imaging and analysis of all samples was performed using an Axon Genepix 4400 tabletop scanner and ImageJ Fiji, as described above.

Surface Adhesion of Cells.

NIH 3T3 fibroblast cells stably expressing GFP (3T3-GFP) were acquired from Cell BioLabs Inc. Cells were cultured in Dulbecco's Modified Eagle Medium (DMEM) supplemented with 10% fetal bovine serum and kept in a tissue culture incubator at 37°C and 5% CO_2. Cells were harvested by trypsinization, counted, and then 3×10^6 cells were re-seeded onto POEGMA brush-coated slides placed in quadriPERM® slide cell culture chambers (Sarstedt AG & Co). After a 24 h incubation period, the surfaces were gently rinsed 3 times and placed in culture dishes containing fresh growth medium. Epifluorescence imaging under the GFP channel was performed using a Nikon TE2000 inverted microscope. Images were analyzed with ImageJ Fiji via intensity thresholding to calculate the percentage of pixels in the field of view showing positive signal in the GFP channel (% FOV) as a metric for surface coverage by 3T3-GFP cells.

Microarray-based indirect sandwich immunoassays (ISIAs) against anti-HIV p24 Abs on POEGMA.

(A) anti-APA ISIA: Microarrays of PEGylated BSA (Life Diagnostics PBSA-00) were prepared by printing onto surfaces with a noncontact microarray printer (Scienion sciFlEXARRAYER S11) at a concentration of 1 mg/mL as microspots and then placed in a vacuum dessicator overnight. Next, these assays were run against serial dilutions of pAPA1 (ThermoFisher PA5–32247) spiked into calf serum and incubated for 1 h. The surfaces were then washed 3 times and then exposed to a 1 μg/mL solution of Cy5-donkey-anti-rabbit antibody (R&D Systems) for 30 min. Surfaces were then rinsed again to remove any unbound proteins, centrifuged at 4800 rpm for 15 s to wick away excess liquid, then allowed to dry under ambient conditions. Fluorescence imaging of all samples was performed using an Axon Genepix 4400 tabletop scanner as described above. *(B) anti-HIV p24 ISIA:* Recombinant HIV p24 Ag (Advanced Biotechnologies Inc. #14–101-050) was printed onto surfaces with a noncontact microarray printer as described above. Next, serial dilutions of rabbit-anti-p24 Abs (Sigma Aldrich SAB3500946) spiked into calf serum were applied to printed microarrays and incubated for 1 h. Simultaneously, a similar set of dilution series

was run in parallel, except here the samples also contained 100 ng/mL of rabbit-derived pAPA1 (ThermoFisher PA5–32247) acting as an interferent. Samples were subsequently processed and imaged as described above.

Assessment of anti-PEG reactivity in patient samples.

The patients from whom these samples were obtained were in a clinical trial conducted under Duke University IRB Protocol #577-04-4. Informed signed consent was obtained from either the patient or from next of kin. *(A) ELISA detection of APAs:* Plasma samples diluted 1:21 in 1% BSA in PBS were tested by ELISA for IgG Ab to PEG essentially as described previously [11, 12, 14], but using Adagen® (Sigma Tau Pharmaceuticals, Gaithersburg, MD) rather than Krystexxa® as the antigen. *(B) Surface fluoroimmunoassay against patient APAs:* Polymer-coated surfaces were incubated with patient plasma samples diluted 1:3 in PBS for 1 h, and then washed 3 times with wash buffer (0.5% CHAPS in PBS). Next, the surfaces were exposed to a 1 μg/mL solution of Cy5-goat-anti-human IgG detection Ab (R & D Systems, Inc.) for 30 min. Surfaces were then rinsed again to remove any loosely-bound proteins, centrifuged at 4800 rpm for 15 s to wick away excess liquid, then allowed to dry under ambient conditions. Fluorescence imaging and analysis of all samples was performed using an Axon Genepix 4400 tabletop scanner and ImageJ Fiji as described above.

Statistical Analysis.

Statistical analyses were performed by Graphpad Prism 6 (San Diego, CA). Results are plotted as mean ± 95% CI (Figures 1d, 2c, 3c, 3f, S4) or as mean ± s.d. (Figures 4c, 4e, 4g, 5c–f, 6, S2, S3, and S6). Sample sizes are included in figure captions. Differences between groups were analyzed by one-way or two-way ANOVA analysis (as indicated in caption) followed by Tukey's post hoc test. For all statistical analyses, $p < 0.05$ was used as the threshold for significance.

Supplementary Material

Refer to Web version on PubMed Central for supplementary material.

ACKNOWLEDGEMENTS

The authors thank John Horton and Dr. Raluca Gordan for technical support with microarray imaging. DYJ was supported by the Duke Medical Scientist Training Program (T32GM007171). The authors gratefully acknowledge funding support from National Cancer Institute Grant 1UG3CA211232-01, Department of Defense United States Special Operations Command Grant W81XWH-16-C-0219 and Combat Casualty Care Research Program (JPC-6) Grant W81XWH-17-2-0045. Funding support was also received from Duke-Coulter Translational Partnership. The content reflects the views of the authors and does not necessarily represent the official views of the supporting organizations.

REFERENCES

1. Zhang P, Sun F, Liu S, Jiang S. Anti-PEG antibodies in the clinic: Current issues and beyond PEGylation. Journal of controlled release : official journal of the Controlled Release Society. 2016;244(Pt B):184–93. Epub 2016/07/03. doi: 10.1016/j.jconrel.2016.06.040 PubMed PMID: ; PMCID: PMC5747248. [PubMed: 27369864]

2. Abuchowski A, McCoy JR, Palczuk NC, van Es T, Davis FF. Effect of covalent attachment of polyethylene glycol on immunogenicity and circulating life of bovine liver catalase. The Journal of biological chemistry. 1977;252(11):3582–6. Epub 1977/06/10. PubMed PMID: . [PubMed: 16907]

3. Abuchowski A, van Es T, Palczuk NC, Davis FF. Alteration of immunological properties of bovine serum albumin by covalent attachment of polyethylene glycol. The Journal of biological chemistry. 1977;252(11):3578–81. Epub 1977/06/10. PubMed PMID: . [PubMed: 405385]

4. Coatings for Biomedical Applications. 1st Edition ed. Driver M, editor. Cambridge, United Kingdon: Woodhead Publishing; 2012.

5. Hucknall A, Rangarajan S, Chilkoti A. In Pursuit of Zero: Polymer Brushes that Resist the Adsorption of Proteins. Advanced Materials. 2009;21(23):2441–6. doi: 10.1002/adma.200900383.

6. Ni S, Yao H, Wang L, Lu J, Jiang F, Lu A, Zhang G. Chemical Modifications of Nucleic Acid Aptamers for Therapeutic Purposes. International journal of molecular sciences. 2017;18(8). Epub 2017/08/03. doi: 10.3390/ijms18081683 PubMed PMID: ; PMCID: PMC5578073. [PubMed: 28767098]

7. Swierczewska M, Lee KC, Lee S. What is the future of PEGylated therapies? Expert opinion on emerging drugs. 2015;20(4):531–6. Epub 2015/11/20. doi: 10.1517/14728214.2015.1113254 PubMed PMID: ; PMCID: PMC4908577. [PubMed: 26583759]

8. Richter AW, Akerblom E. Antibodies against polyethylene glycol produced in animals by immunization with monomethoxy polyethylene glycol modified proteins. International archives of allergy and applied immunology. 1983;70(2):124–31. Epub 1983/01/01. PubMed PMID: . [PubMed: 6401699]

9. Sroda K, Rydlewski J, Langner M, Kozubek A, Grzybek M, Sikorski AF. Repeated injections of PEG-PE liposomes generate anti-PEG antibodies. Cellular & molecular biology letters. 2005;10(1): 37–47. Epub 2005/04/06. PubMed PMID: . [PubMed: 15809678]

10. Cheng TL, Cheng CM, Chen BM, Tsao DA, Chuang KH, Hsiao SW, Lin YH, Roffler SR. Monoclonal antibody-based quantitation of poly(ethylene glycol)-derivatized proteins, liposomes, and nanoparticles. Bioconjugate chemistry. 2005;16(5):1225–31. Epub 2005/09/22. doi: 10.1021/bc050133f PubMed PMID: . [PubMed: 16173802]

11. Ganson NJ, Kelly SJ, Scarlett E, Sundy JS, Hershfield MS. Control of hyperuricemia in subjects with refractory gout, and induction of antibody against poly(ethylene glycol) (PEG), in a phase I trial of subcutaneous PEGylated urate oxidase. Arthritis research & therapy. 2006;8(1):R12-R. doi: 10.1186/ar1861 PubMed PMID: .

12. Hershfield MS, Ganson NJ, Kelly SJ, Scarlett EL, Jaggers DA, Sundy JS. Induced and pre-existing anti-polyethylene glycol antibody in a trial of every 3-week dosing of pegloticase for refractory gout, including in organ transplant recipients. Arthritis research & therapy. 2014;16(2):R63. Epub 2014/03/08. doi: 10.1186/ar4500 PubMed PMID: 24602182; PMCID: .

13. Armstrong JK, Hempel G, Koling S, Chan LS, Fisher T, Meiselman HJ, Garratty G. Antibody against poly(ethylene glycol) adversely affects PEG-asparaginase therapy in acute lymphoblastic leukemia patients. Cancer. 2007;110(1):103–11. Epub 2007/05/23. doi: 10.1002/cncr.22739 PubMed PMID: . [PubMed: 17516438]

14. Ganson NJ, Povsic TJ, Sullenger BA, Alexander JH, Zelenkofske SL, Sailstad JM, Rusconi CP, Hershfield MS. Pre-existing anti–polyethylene glycol antibody linked to first-exposure allergic reactions to pegnivacogin, a PEGylated RNA aptamer. Journal of Allergy and Clinical Immunology. 2016;137(5):1610–3.e7. doi: 10.1016/j.jaci.2015.10.034. [PubMed: 26688515]

15. Povsic TJ, Lawrence MG, Lincoff AM, Mehran R, Rusconi CP, Zelenkofske SL, Huang Z, Sailstad J, Armstrong PW, Steg PG, Bode C, Becker RC, Alexander JH, Adkinson NF, Levinson AI. Pre-existing anti-PEG antibodies are associated with severe immediate allergic reactions to pegnivacogin, a PEGylated aptamer. Journal of Allergy and Clinical Immunology. 2016;138(6): 1712–5. doi: 10.1016/j.jaci.2016.04.058. [PubMed: 27522158]

16. Sundy JS, Baraf HS, Yood RA, Edwards NL, Gutierrez-Urena SR, Treadwell EL, Vazquez-Mellado J, White WB, Lipsky PE, Horowitz Z, Huang W, Maroli AN, Waltrip RW 2nd, Hamburger SA, Becker MA Efficacy and tolerability of pegloticase for the treatment of chronic gout in patients refractory to conventional treatment: two randomized controlled trials. Jama. 2011;306(7):711–20. Epub 2011/08/19. doi: 10.1001/jama.2011.1169 PubMed PMID: . [PubMed: 21846852]

17. Verhoef JJF, Carpenter JF, Anchordoquy TJ, Schellekens H. Potential induction of anti-PEG antibodies and complement activation toward PEGylated therapeutics. Drug Discovery Today. 2014;19(12):1945–52. doi: 10.1016/j.drudis.2014.08.015. [PubMed: 25205349]

18. Rau RE, Dreyer Z, Choi MR, Liang W, Skowronski R, Allamneni KP, Devidas M, Raetz EA, Adamson PC, Blaney SM, Loh ML, Hunger SP. Outcome of pediatric patients with acute lymphoblastic leukemia/lymphoblastic lymphoma with hypersensitivity to pegaspargase treated with PEGylated Erwinia asparaginase, pegcrisantaspase: A report from the Children's Oncology Group. Pediatric blood & cancer. 2018;65(3). Epub 2017/11/02. doi: 10.1002/pbc.26873 PubMed PMID: ; PMCID: PMC5839116. [PubMed: 29090524]

19. Longo N, Harding CO, Burton BK, Grange DK, Vockley J, Wasserstein M, Rice GM, Dorenbaum A, Neuenburg JK, Musson DG, Gu Z, Sile S. Single-dose, subcutaneous recombinant phenylalanine ammonia lyase conjugated with polyethylene glycol in adult patients with phenylketonuria: an open-label, multicentre, phase 1 dose-escalation trial. Lancet (London, England). 2014;384(9937):37–44. Epub 2014/04/20. doi: 10.1016/s0140-6736(13)61841-3 PubMed PMID: ; PMCID: PMC4447208. [PubMed: 24743000]

20. Yang Q, Jacobs TM, McCallen JD, Moore DT, Huckaby JT, Edelstein JN, Lai SK. Analysis of Pre-existing IgG and IgM Antibodies against Polyethylene Glycol (PEG) in the General Population. Analytical Chemistry. 2016;88(23):11804–12. doi: 10.1021/acs.analchem.6b03437. [PubMed: 27804292]

21. Chen B-M, Su Y-C, Chang C-J, Burnouf P-A, Chuang K-H, Chen C-H, Cheng T-L, Chen Y-T, Wu J-Y, Roffler SR. Measurement of Pre-Existing IgG and IgM Antibodies against Polyethylene Glycol in Healthy Individuals. Analytical Chemistry. 2016;88(21):10661–6. doi: 10.1021/acs.analchem.6b03109. [PubMed: 27726379]

22. Guidance for Industry: Immunogenicity Assessment for Therapeutic Proteins. In: U.S. Department of Health and Human Services FaDA, editor. 2014.

23. Jiang S, Cao Z. Ultralow-Fouling, Functionalizable, and Hydrolyzable Zwitterionic Materials and Their Derivatives for Biological Applications. Advanced Materials. 2010;22(9):920–32. doi: 10.1002/adma.200901407. [PubMed: 20217815]

24. Zhang P, Sun F, Tsao C, Liu S, Jain P, Sinclair A, Hung H-C, Bai T, Wu K, Jiang S. Zwitterionic gel encapsulation promotes protein stability, enhances pharmacokinetics, and reduces immunogenicity. Proceedings of the National Academy of Sciences of the United States of America. 2015;112(39):12046–51. doi: 10.1073/pnas.1512465112 PubMed PMID: . [PubMed: 26371311]

25. Mero A, Fang Z, Pasut G, Veronese FM, Viegas TX. Selective conjugation of poly(2-ethyl 2-oxazoline) to granulocyte colony stimulating factor. Journal of Controlled Release. 2012;159(3):353–61. doi: 10.1016/j.jconrel.2012.02.025. [PubMed: 22405905]

26. Specht C, Schluter B, Rolfing M, Bruning K, Pauels HG, Kolsch E. Idiotype-specific CD4(+)CD25(+) T suppressor cells prevent, by limiting antibody diversity, the occurrence of anti-dextran antibodies crossreacting with histone H3. European Journal of Immunology. 2003;33(5):1242–9. doi: 10.1002/eji.200323273 PubMed PMID: WOS:. [PubMed: 12731049]

27. Soshee A, Zurcher S, Spencer ND, Halperin A, Nizak C. General In Vitro Method to Analyze the Interactions of Synthetic Polymers with Human Antibody Repertoires. Biomacromolecules. 2014;15(1):113–21. doi: 10.1021/bm401360y PubMed PMID: WOS:. [PubMed: 24328191]

28. McCallen J, Prybylski J, Yang Q, Lai SK. Cross-Reactivity of Select PEG-Binding Antibodies to Other Polymers Containing a C-C-O Backbone. ACS Biomaterials Science & Engineering. 2017;3(8):1605–15. doi: 10.1021/acsbiomaterials.7b00147.

29. Fernandez CA, Stewart E, Panetta JC, Wilkinson MR, Morrison AR, Finkelman FD, Sandlund JT, Pui CH, Jeha S, Relling MV, Campbell PK. Successful challenges using native E. coli asparaginase after hypersensitivity reactions to PEGylated E. coli asparaginase. Cancer chemotherapy and pharmacology. 2014;73(6):1307–13. doi: 10.1007/s00280-014-2464-2 PubMed PMID: . [PubMed: 24771103]

30. Pui CH, Liu Y, Relling MV. How to solve the problem of hypersensitivity to asparaginase? Pediatric blood & cancer. 2018;65(3). Epub 2017/11/23. doi: 10.1002/pbc.26884 PubMed PMID: ; PMCID: PMC5766401. [PubMed: 29165928]

31. Lee PW, Isarov SA, Wallat JD, Molugu SK, Shukla S, Sun JEP, Zhang J, Zheng Y, Lucius Dougherty M, Konkolewicz D, Stewart PL, Steinmetz NF, Hore MJA, Pokorski JK. Polymer Structure and Conformation Alter the Antigenicity of Virus-like Particle–Polymer Conjugates. Journal of the American Chemical Society. 2017;139(9):3312–5. doi: 10.1021/jacs.6b11643. [PubMed: 28121424]
32. Qi Y, Simakova A, Ganson NJ, Li X, Luginbuhl KM, Ozer I, Liu W, Hershfield MS, Matyjaszewski K, Chilkoti A. A brush-polymer/exendin-4 conjugate reduces blood glucose levels for up to five days and eliminates poly(ethylene glycol) antigenicity2016;1:0002. doi: 10.1038/s41551-016-0002 http://dharmasastra.live.cf.private.springer.com/articles/s41551-016-0002#supplementary-information.
33. Liu M, Johansen P, Zabel F, Leroux JC, Gauthier MA. Semi-permeable coatings fabricated from comb-polymers efficiently protect proteins in vivo. Nature communications. 2014;5:5526. Epub 2014/11/20. doi: 10.1038/ncomms6526 PubMed PMID: . [PubMed: 25407758]
34. Nguyen TH, Kim S-H, Decker CG, Wong DY, Loo JA, Maynard HD. A Heparin-Mimicking Polymer Conjugate Stabilizes Basic Fibroblast Growth Factor (bFGF). Nature chemistry. 2013;5(3):221–7. doi: 10.1038/nchem.1573 PubMed PMID: .
35. Krishnamoorthy M, Hakobyan S, Ramstedt M, Gautrot JE. Surface-initiated polymer brushes in the biomedical field: applications in membrane science, biosensing, cell culture, regenerative medicine and antibacterial coatings. Chemical reviews. 2014;114(21):10976–1026. Epub 2014/10/30. doi: 10.1021/cr500252u PubMed PMID: . [PubMed: 25353708]
36. Hucknall A, Simnick AJ, Hill RT, Chilkoti A, Garcia A, Johannes MS, Clark RL, Zauscher S, Ratner BD. Versatile synthesis and micropatterning of nonfouling polymer brushes on the wafer scale. Biointerphases. 2009;4(2):Fa50–7. Epub 2010/04/23. doi: 10.1116/1.3151968 PubMed PMID: . [PubMed: 20408717]
37. Hucknall A, Kim DH, Rangarajan S, Hill RT, Reichert WM, Chilkoti A. Simple Fabrication of Antibody Microarrays on Nonfouling Polymer Brushes with Femtomolar Sensitivity for Protein Analytes in Serum and Blood. Advanced Materials. 2009;21(19):1968–71. doi: 10.1002/adma.200803125 PubMed PMID: ISI:. [PubMed: 31097880]
38. Joh DY, Hucknall AM, Wei Q, Mason KA, Lund ML, Fontes CM, Hill RT, Blair R, Zimmers Z, Achar RK, Tseng D, Gordan R, Freemark M, Ozcan A, Chilkoti A. Inkjet-printed point-of-care immunoassay on a nanoscale polymer brush enables subpicomolar detection of analytes in blood. Proceedings of the National Academy of Sciences. 2017;114(34):E7054–E62.
39. Joh DY, McGuire F, Abedini-Nassab R, Andrews JB, Achar RK, Zimmers Z, Mozhdehi D, Blair R, Albarghouthi F, Oles W, Richter J, Fontes CM, Hucknall AM, Yellen BB, Franklin AD, Chilkoti A. Poly(oligo(ethylene glycol) methyl ether methacrylate) Brushes on High-κ Metal Oxide Dielectric Surfaces for Bioelectrical Environments. ACS applied materials & interfaces. 2017;9(6):5522–9. doi: 10.1021/acsami.6b15836. [PubMed: 28117566]
40. Ahmad SA, Leggett GJ, Hucknall A, Chilkoti A. Micro- and nanostructured poly[oligo(ethylene glycol)methacrylate] brushes grown from photopatterned halogen initiators by atom transfer radical polymerization. Biointerphases. 2011;6(1):8–15. doi: 10.1116/1.3553579 PubMed PMID: . [PubMed: 21428690]
41. Ma H, Li D, Sheng X, Zhao B, Chilkoti A. Protein-resistant polymer coatings on silicon oxide by surface-initiated atom transfer radical polymerization. Langmuir : the ACS journal of surfaces and colloids. 2006;22(8):3751–6. Epub 2006/04/06. doi: 10.1021/la052796r PubMed PMID: . [PubMed: 16584252]
42. Welch ME, Ritzert NL, Chen H, Smith NL, Tague ME, Xu Y, Baird BA, Abruña HD, Ober CK. Generalized Platform for Antibody Detection using the Antibody Catalyzed Water Oxidation Pathway. Journal of the American Chemical Society. 2014;136(5):1879–83. doi: 10.1021/ja409598c. [PubMed: 24410628]
43. Harrison RH, Steele JA, Chapman R, Gormley AJ, Chow LW, Mahat MM, Podhorska L, Palgrave RG, Payne DJ, Hettiaratchy SP, Dunlop IE, Stevens MM. Modular and Versatile Spatial Functionalization of Tissue Engineering Scaffolds through Fiber-Initiated Controlled Radical Polymerization. Adv Funct Mater. 2015;25(36):5748–57. Epub 2016/05/03. doi: 10.1002/adfm.201501277 PubMed PMID: 27134621; PMCID: . [PubMed: 27134621]

44. Ma H, Wells M, Beebe TP, Chilkoti A. Surface-Initiated Atom Transfer Radical Polymerization of Oligo(ethylene glycol) Methyl Methacrylate from a Mixed Self-Assembled Monolayer on Gold. Advanced Functional Materials. 2006;16(5):640–8. doi: 10.1002/adfm.200500426.
45. Ma H, Hyun J, Stiller P, Chilkoti A. "Non-Fouling" Oligo(ethylene glycol)- Functionalized Polymer Brushes Synthesized by Surface-Initiated Atom Transfer Radical Polymerization. Advanced Materials. 2004;16(4):338–41. doi: 10.1002/adma.200305830.
46. Verduzco R, Li X, Pesek SL, Stein GE. Structure, function, self-assembly, and applications of bottlebrush copolymers. Chemical Society Reviews. 2015;44(8):2405–20. doi: 10.1039/C4CS00329B. [PubMed: 25688538]
47. Lee KC, Lee S. Drug delivery: Brushing off antigenicity. Nature Biomedical Engineering. 2017;1:0019. doi: 10.1038/s41551-016-0019.
48. Feng W, Zhu S, Ishihara K, Brash JL. Protein resistant surfaces: comparison of acrylate graft polymers bearing oligo-ethylene oxide and phosphorylcholine side chains. Biointerphases. 2006;1(1):50. Epub 2006/03/01. doi: 10.1116/1.2187495 PubMed PMID: . [PubMed: 20408615]
49. Jin Z, Feng W, Beisser K, Zhu S, Sheardown H, Brash JL. Protein-resistant polyurethane prepared by surface-initiated atom transfer radical graft polymerization (ATRgP) of water-soluble polymers: effects of main chain and side chain lengths of grafts. Colloids and surfaces B, Biointerfaces. 2009;70(1):53–9. Epub 2009/01/20. doi: 10.1016/j.colsurfb.2008.12.005 PubMed PMID: . [PubMed: 19150594]
50. Lee BS, Chi YS, Lee KB, Kim YG, Choi IS. Functionalization of poly(oligo(ethylene glycol) methacrylate) films on gold and Si/SiO2 for immobilization of proteins and cells: SPR and QCM studies. Biomacromolecules. 2007;8(12):3922–9. Epub 2007/11/28. doi: 10.1021/bm7009043 PubMed PMID: . [PubMed: 18039000]
51. Gautrot JE, Trappmann B, Oceguera-Yanez F, Connelly J, He X, Watt FM, Huck WT. Exploiting the superior protein resistance of polymer brushes to control single cell adhesion and polarisation at the micron scale. Biomaterials. 2010;31(18):5030–41. Epub 2010/03/30. doi: 10.1016/j.biomaterials.2010.02.066 PubMed PMID: ; PMCID: Pmc3712172. [PubMed: 20347135]
52. Simakova A, Averick SE, Konkolewicz D, Matyjaszewski K. Aqueous ARGET ATRP. Macromolecules. 2012;45(16):6371–9. doi: 10.1021/ma301303b.
53. Panzarasa G, Soliveri G, Sparnacci K, Ardizzone S. Patterning of polymer brushes made easy using titanium dioxide: direct and remote photocatalytic lithography. Chemical Communications. 2015;51(34):7313–6. doi: 10.1039/C5CC00255A. [PubMed: 25820627]
54. Edmondson S, Osborne VL, Huck WTS. Polymer brushes via surface-initiated polymerizations. Chemical Society Reviews. 2004;33(1):14–22. doi: 10.1039/B210143M. [PubMed: 14737505]
55. Heide Pvd. X-Ray Photoelectron Spectroscopy: An Introduction to Principles and Practices. Hoboken, NJ: John Wiley and Sons; 2011.
56. Sherman MR, Saifer MGP, David Williams L, Michaels SJ, Sobczyk MA. Next-generation PEGylation enables reduced immunoreactivity of PEG-protein conjugates. Drug Development and Delivery. 2012;12(5):36–42.
57. Sherman MR, Williams LD, Sobczyk MA, Michaels SJ, Saifer MG. Role of the methoxy group in immune responses to mPEG-protein conjugates. Bioconjugate chemistry. 2012;23(3):485–99. Epub 2012/02/16. doi: 10.1021/bc200551b PubMed PMID: ; PMCID: PMC3309606. [PubMed: 22332808]
58. Ilinskaya AN, Dobrovolskaia MA. Understanding the immunogenicity and antigenicity of nanomaterials: Past, present and future. Toxicology and applied pharmacology. 2016;299:70–7. doi: 10.1016/j.taap.2016.01.005 PubMed PMID: . [PubMed: 26773813]
59. Zhu J, Liu D, He C. Enhanced antifouling ability of a poly(vinylidene fluoride) membrane functionalized with a zwitterionic serine-based layer. RSC Advances. 2016;6(88):85612–20. doi: 10.1039/C6RA19067G.
60. Saifer MGP, Williams LD, Sobczyk MA, Michaels SJ, Sherman MR. Selectivity of binding of PEGs and PEG-like oligomers to anti-PEG antibodies induced by methoxyPEG-proteins. Molecular Immunology. 2014;57(2):236–46. doi: 10.1016/j.molimm.2013.07.014. [PubMed: 24200843]

61. Fontes CM, Achar RK, Joh DY, Ozer I, Bhattacharjee S, Hucknall A, Chilkoti A. Engineering the Surface Properties of a Zwitterionic Polymer Brush to Enable the Simple Fabrication of Inkjet-Printed Point-of-Care Immunoassays. Langmuir : the ACS journal of surfaces and colloids. 2019;35(5):1379–90. Epub 2018/08/09. doi: 10.1021/acs.langmuir.8b01597 PubMed PMID: . [PubMed: 30086642]
62. Martinez Alexa L, Sherman Merry R, Saifer Mark GP, Williams LD, inventorsPolymer Conjugates With Decreased Antigenicity, Methods Of Preparation And Uses Thereof. US patent US 8129330 B2. 2012 2003/09/25.
63. Zhang P, Sun F, Hung HC, Jain P, Leger KJ, Jiang S. Sensitive and Quantitative Detection of Anti-Poly(ethylene glycol) (PEG) Antibodies by Methoxy-PEG-Coated Surface Plasmon Resonance Sensors. Anal Chem. 2017;89(16):8217–22. Epub 2017/07/21. doi: 10.1021/acs.analchem.7b02447 PubMed PMID: ; PMCID: PMC5750323. [PubMed: 28727918]
64. Harder P, Grunze M, Dahint R, Whitesides GM, Laibinis PE. Molecular Conformation in Oligo(ethylene glycol)-Terminated Self-Assembled Monolayers on Gold and Silver Surfaces Determines Their Ability To Resist Protein Adsorption. The Journal of Physical Chemistry B. 1998;102(2):426–36. doi: 10.1021/jp972635z.
65. Capadona JR, Collard DM, García AJ. Fibronectin Adsorption and Cell Adhesion to Mixed Monolayers of Tri(ethylene glycol)- and Methyl-Terminated Alkanethiols. Langmuir : the ACS journal of surfaces and colloids. 2003;19(5):1847–52. doi: 10.1021/la026244+.
66. Zhu B, Eurell T, Gunawan R, Leckband D. Chain-length dependence of the protein and cell resistance of oligo(ethylene glycol)-terminated self-assembled monolayers on gold. Journal of Biomedical Materials Research. 2001;56(3):406–16. doi: 10.1002/1097-4636(20010905)56:3<406::AID-JBM1110>3.0.CO;2-R. [PubMed: 11372059]
67. Schellekens H, Hennink WE, Brinks V. The immunogenicity of polyethylene glycol: facts and fiction. Pharmaceutical research. 2013;30(7):1729–34. Epub 2013/05/16. doi: 10.1007/s11095-013-1067-7 PubMed PMID: . [PubMed: 23673554]
68. McSweeney Morgan D, Versfeld Zina C, Carpenter Delesha M, Lai Samuel K. Physician Awareness of Immune Responses to Polyethylene Glycol-Drug Conjugates. Clinical and Translational Science. 2018;11(2):162–5. doi: 10.1111/cts.12537. [PubMed: 29383836]
69. Lipsky PE, Calabrese LH, Kavanaugh A, Sundy JS, Wright D, Wolfson M, Becker MA. Pegloticase immunogenicity: the relationship between efficacy and antibody development in patients treated for refractory chronic gout. Arthritis research & therapy. 2014;16(2):R60. doi: 10.1186/ar4497. [PubMed: 24588936]
70. Zhou L, Hoofring SA, Wu Y, Vu T, Ma P, Swanson SJ, Chirmule N, Starcevic M. Stratification of Antibody-Positive Subjects by Antibody Level Reveals an Impact of Immunogenicity on Pharmacokinetics. The AAPS Journal. 2013;15(1):30–40. doi: 10.1208/s12248-012-9408-8 PubMed PMID: . [PubMed: 23054969]
71. Fairley N, Ltd CS. CasaXPS Manual 2.3.15: CasaXPX Processing Software for XPS Spectra: Casa Software Limited; 2009.
72. Schindelin J, Arganda-Carreras I, Frise E, Kaynig V, Longair M, Pietzsch T, Preibisch S, Rueden C, Saalfeld S, Schmid B, Tinevez JY, White DJ, Hartenstein V, Eliceiri K, Tomancak P, Cardona A. Fiji: an open-source platform for biological-image analysis. Nature methods. 2012;9(7):676–82. Epub 2012/06/30. doi: 10.1038/nmeth.2019 PubMed PMID: ; PMCID: PMC3855844. [PubMed: 22743772]

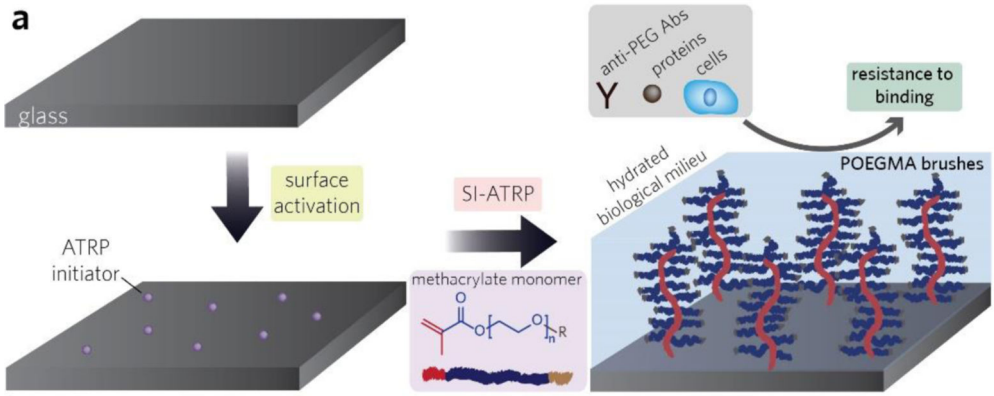

b

Monomer	MW	EG# (n)	R	Abbrev.	Δ (nm)
Ethylene glycol methyl ether methacrylate	144	1	-OMe	EG1-OMe	31.9±4.0
Di(ethylene glycol) methyl ether methacrylate	188	2	-OMe	EG2-OMe	31.5±2.1
Tri(ethylene glycol) methyl ether methacrylate	232	3	-OMe	EG3-OMe	46.5±5.0
Poly(ethylene glycol) methyl ether methacrylate	300	5	-OMe	EG5-OMe	57.9±2.9
Poly(ethylene glycol) methacrylate	360	6	-OH	EG6-OH	28.4±2.4
Poly(ethylene glycol) methyl ether methacrylate	500	9	-OMe	EG9-OMe	52.0±11.8

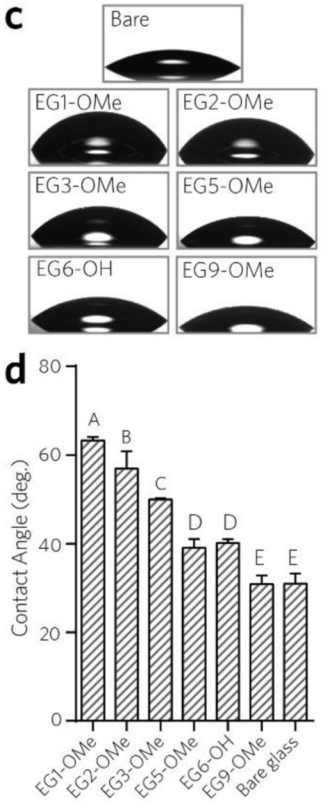

Figure 1 |.

Synthesis of POEGMA bottlebrushes with variable side-chain lengths by surface-initiated atom transfer radical polymerization (SI-ATRP) from planar glass substrates. **a,** Stepwise illustration of POEGMA growth strategy. Glass surfaces are first functionalized ("activated") with a brominated ATRP initiator (see Methods). POEGMA bottlebrushes are then "grafted from" surfaces by SI-ATRP of PEG-methacrylate monomers. **b,** Characteristics of PEG-methacrylate monomers, which were all methoxy-terminated except for the EG6 moiety, which was hydroxy-terminated. (MW = molecular weight, EG# = number of ethylene glycol units, Δ = polymer overlayer thickness in nm). **c, d,** Water contact angle measurement of bottlebrush coatings. Experimental water droplet profiles (**c**) and measured sessile contact angles (**d**) for each surface. Results are plotted as mean ± 95% confidence interval (CI) ($n \geq 3$ per group). Bars marked with a different letter indicates significant differences by multiple comparison testing in one-way ANOVA (Tukey post hoc test, $p \leq 0.05$).

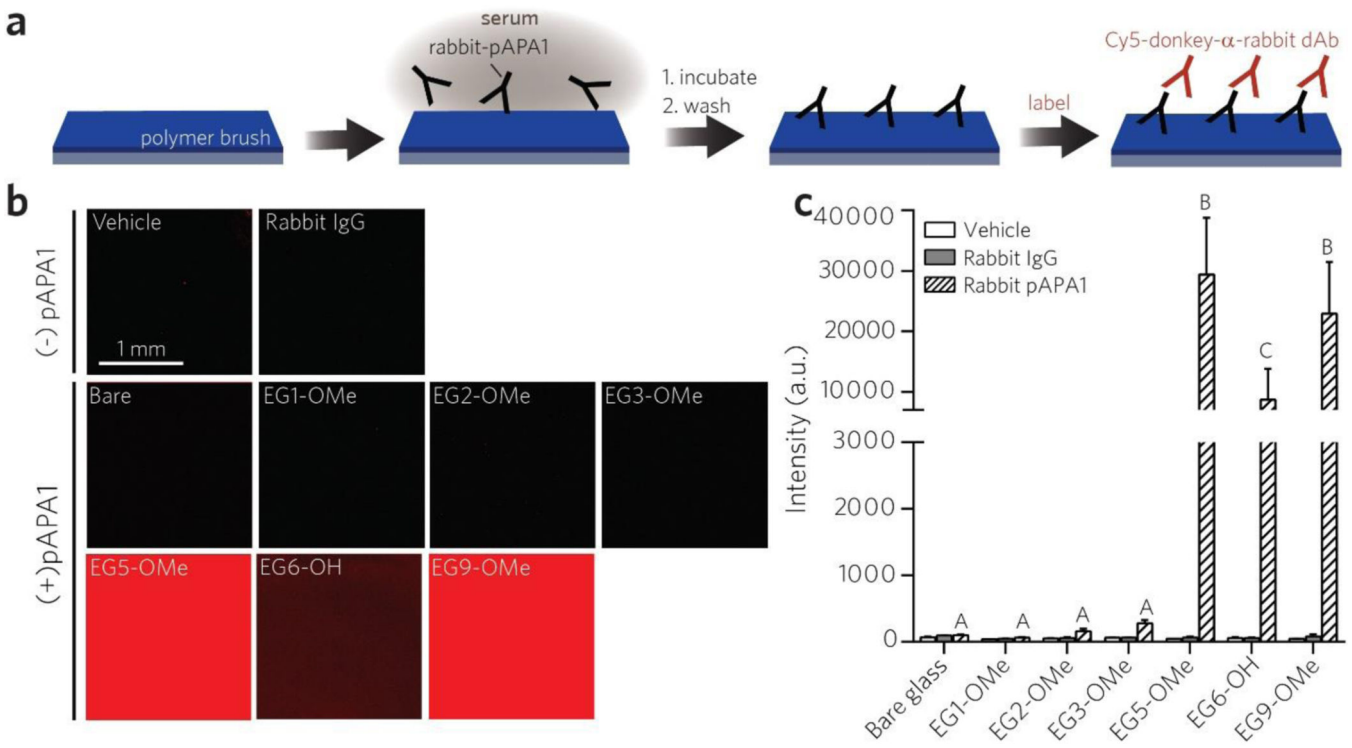

Figure 2 |.

Screening POEGMA bottlebrush surfaces for immune reactivity toward a polyclonal APA (pAPA1). **a,** Schematic of pAPA1 fluoroimmunoassay. Surfaces were incubated with a solution of rabbit-derived pAPA1 spiked into undiluted calf serum, rinsed, and then labeled with Cy5-donkey-α-rabbit dAbs, and then imaged with a fluorescence scanner. **b, c,** Representative Cy5 channel fluorescence images (**b**) and quantitation of mean fluorescence intensities (**c**). Results in (**c**) are plotted as mean ± 95% CI for $n \geq 4$ replicates. Vehicle-only and rabbit-IgG (not specifically reactive to PEG) controls are also included to show baseline values. Incubating surfaces with pAPA1 leads to significant fluorescence, indicating APA binding, from EG5-OMe, EG6-OH, and EG9-OMe surfaces, but not from bare, EG1-OMe, EG2-OM2, or EG3-OMe surfaces. Bars marked with different letters indicate significant differences within the pAPA1-treated groups by multiple comparison testing in one-way ANOVA (Tukey post hoc test, $p \leq 0.05$).

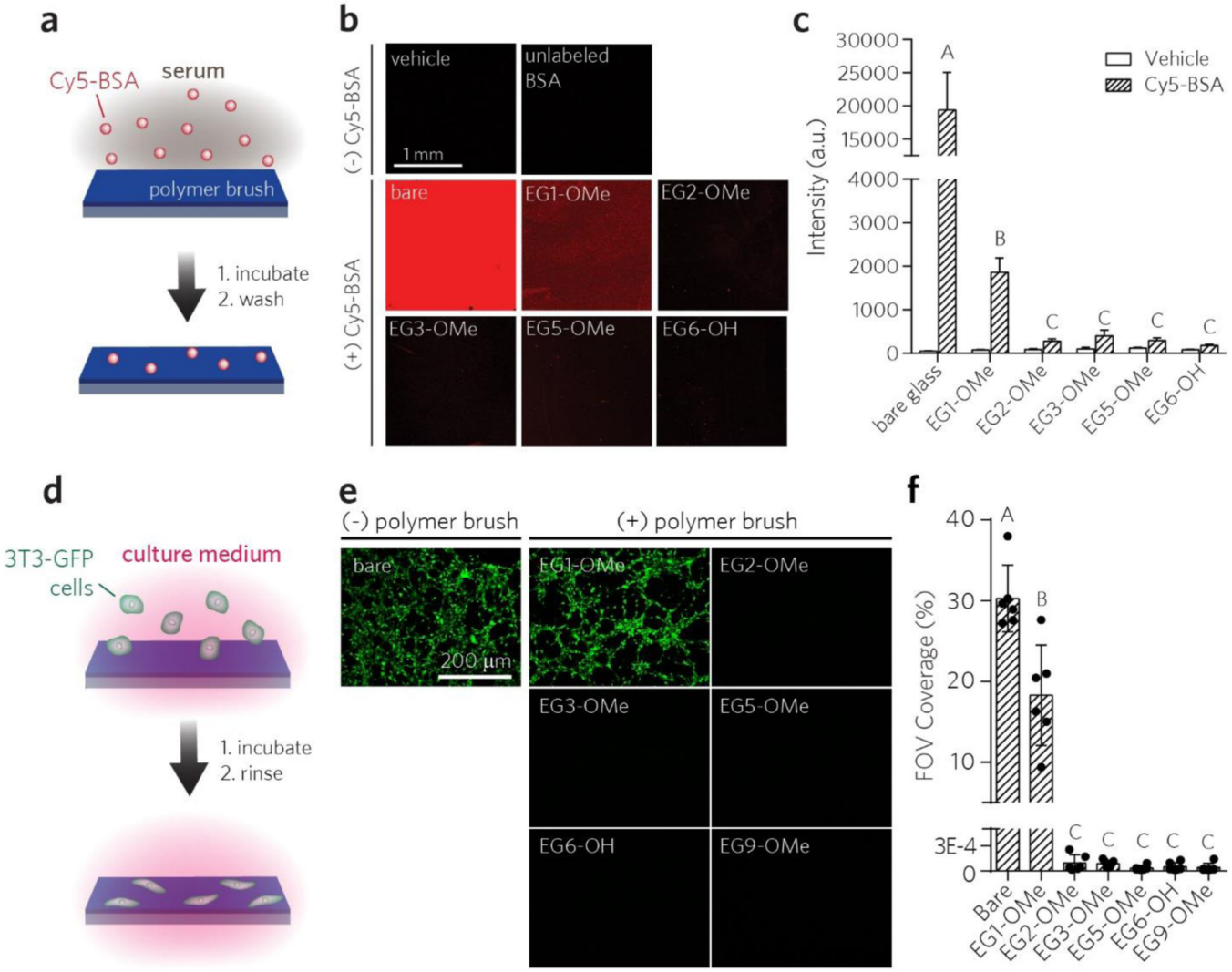

Figure 3 |.

Screening POEGMA brush surfaces for protein adsorption and cell adhesion. **a,** Schematic of surface fluorescence assay used to evaluate protein fouling. Cy5-labeled BSA was incubated on surfaces, rinsed and then read with a scanner for residual fluorescence. **b, c,** Representative Cy5 channel fluorescence images (**b**) and quantitation of mean ± 95% CI fluorescence intensities (**c**) (n = 3 for bare glass, and n ≥ 6 for others). Vehicle groups are plotted for comparison. Bars marked with different letters indicate significant differences within the Cy5-BSA-treated groups by multiple comparison testing in one-way ANOVA (Tukey post hoc test, $p \leq 0.05$). **d,** Schematic of *in vitro* cell adhesion assay. NIH 3T3 cells expressing GFP (3T3-GFP) were incubated on surfaces in complete medium, washed, and then imaged for residual fluorescence on GFP channel by epifluorescence imaging. **e, f,** Representative epifluorescence images of cells (**e**) and quantitation of cell adhesion to surfaces (**f**) expressed as mean %FOV ± 95% CI (n = 6). Bars marked with different letters indicate significantly different groups by multiple comparison testing in one-way ANOVA (Tukey post hoc test, $p \leq 0.05$)

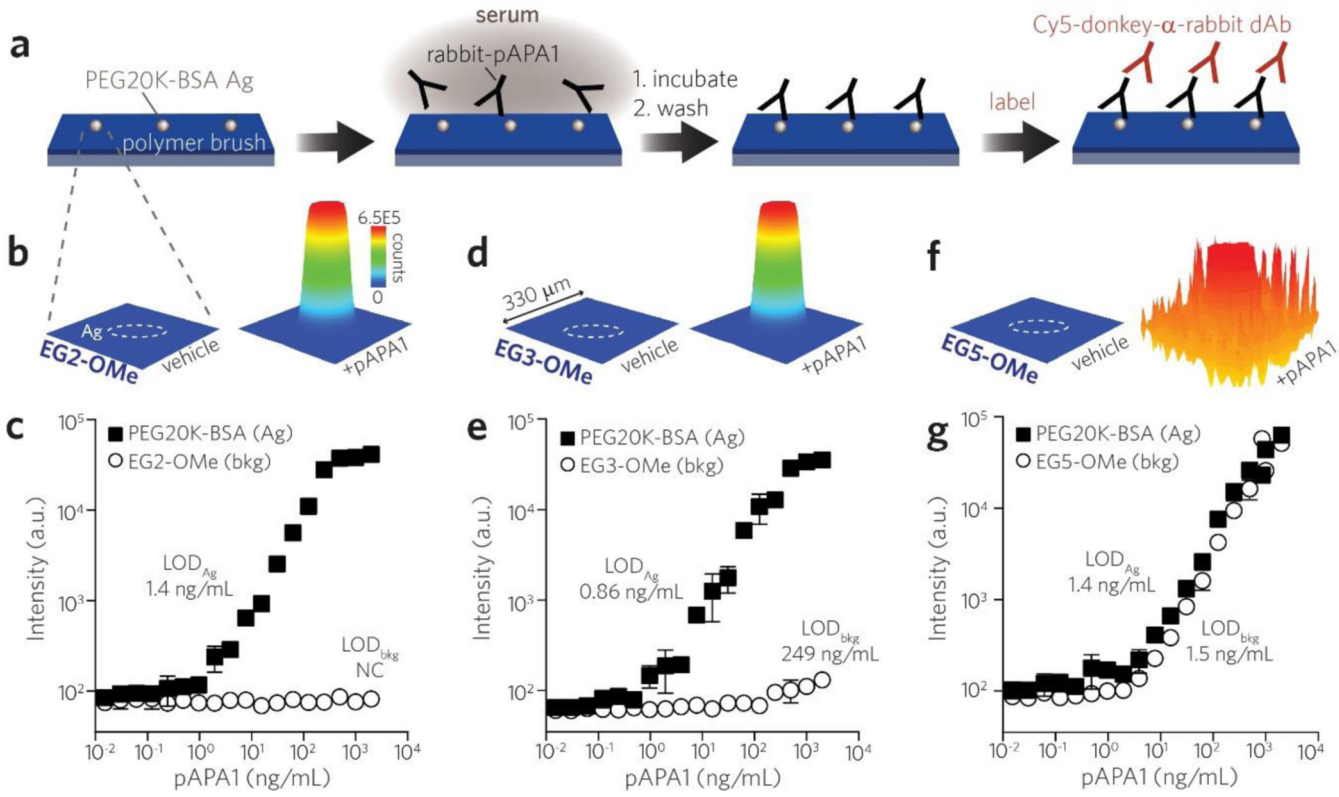

Figure 4 |.

Direct comparison of reactivity of APAs toward POEGMA brushes with different EG sidechain lengths versus linear PEG (MW = 20 K). **a,** Schematic of printing microspots of PEG20K-BSA Ag onto a background of POEGMA brush surfaces. Surfaces were incubated with a dilution series of rabbit-derived pAPA1 in serum, labeled with Cy5-anti-rabbit dAb, and then read by a fluorescence scanner. **b,** Spatial intensity plots of Cy5 fluorescence from EG2-OMe polymer brush surfaces functionalized by PEG20K-BSA Ag microspots (outlined by white dashes). Shown are 330 × 330 μm regions corresponding to surfaces (containing a single Ag microspot) exposed to serum alone (left) versus serum spiked with 2 μg/mL pAPA1 (right). **c,** Concentration curves of pAPA1 binding measured by fluorescence intensity from PEG20K-BSA Ag microspots (black squares) versus that from EG2-OMe POEGMA background (open circles). Similar spatial intensity plots and concentration curves as shown for EG2-OMe in (**b, c**) are shown for EG3-OMe in (**d, e**) and EG5-OMe in (**f, g**). Data plotted in (**c, e, g**) represent mean ± s.d. (n = 3). LODs determined from PEG20K-BSA microspots versus polymer background (LOD_{Ag} vs. LOD_{bkg}, respectively) are displayed adjacent to each curve.

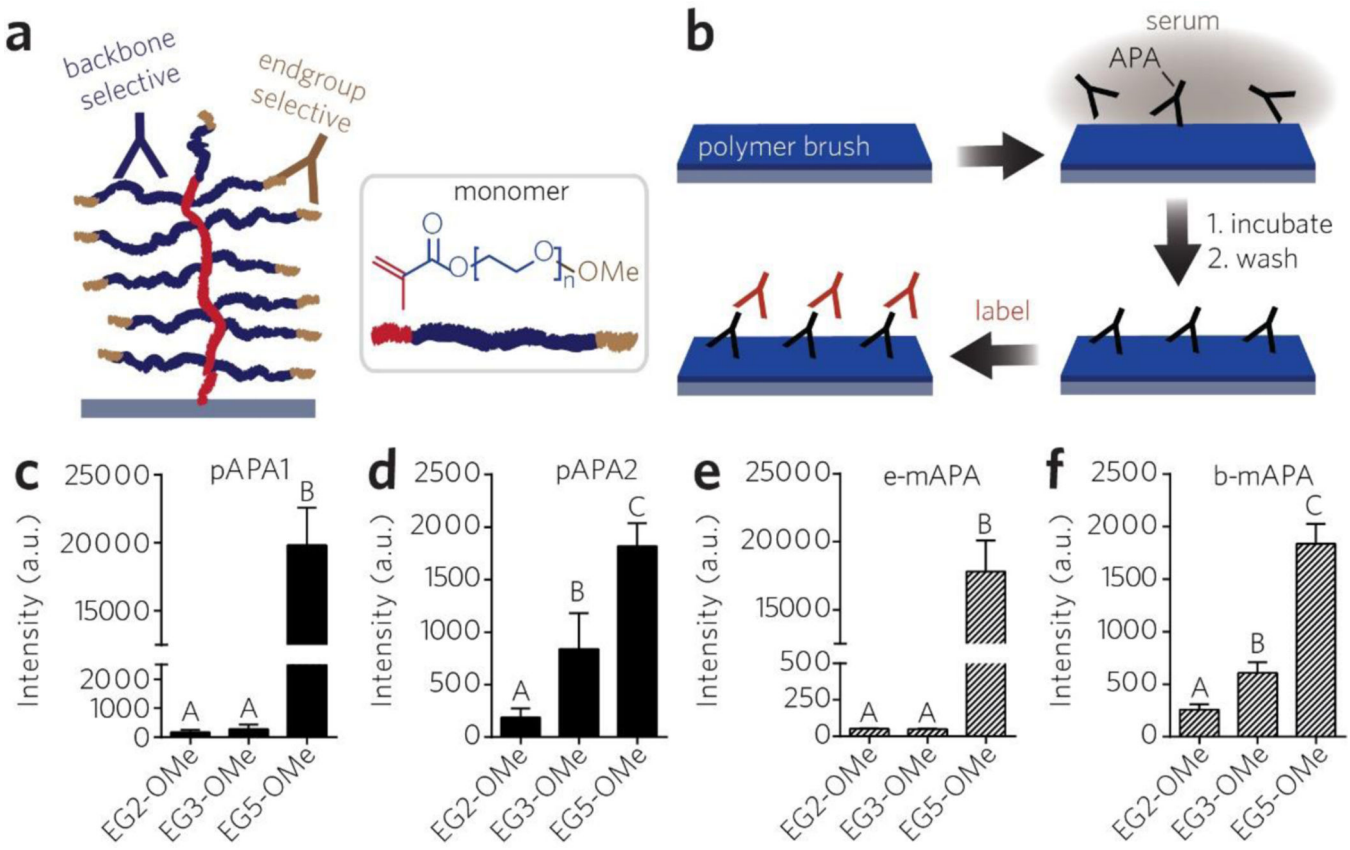

Figure 5 |.

Reactivity of backbone-selective versus endgroup selective APAs toward EG2-OMe, EG3-OMe, and EG5-OMe POEGMA brushes. **a,** Schematic of backbone-selective (blue) versus endgroup-selective (tan) APA binding to PEG backbone and methoxy terminus of a bottlebrush, respectively. **b,** Schematic of surface fluoroimmunoassay for APA binding. Surfaces were incubated with a solution of APA-spiked calf serum, then labeled with Cy5-conjugated dAbs, and then read with a scanner. **c–f,** Reactivity of polyclonal APAs toward bottlebrush surfaces with known selectivity for PEG endgroups (pAPA1) versus backbone (pAPA2) (**c**, **d**), and similar plots shown for endgroup-selective (e-mAPA) versus backbone-selective (b-mAPA) monoclonal APAs (**e**, **f**) as assessed by surface fluoroimmunoassays. Data are plotted as mean fluorescence intensities ± s.d. (n = 9). Bars marked with different letters indicate significant differences by multiple comparison testing in one-way ANOVA (Tukey post hoc test, $p \leq 0.05$).

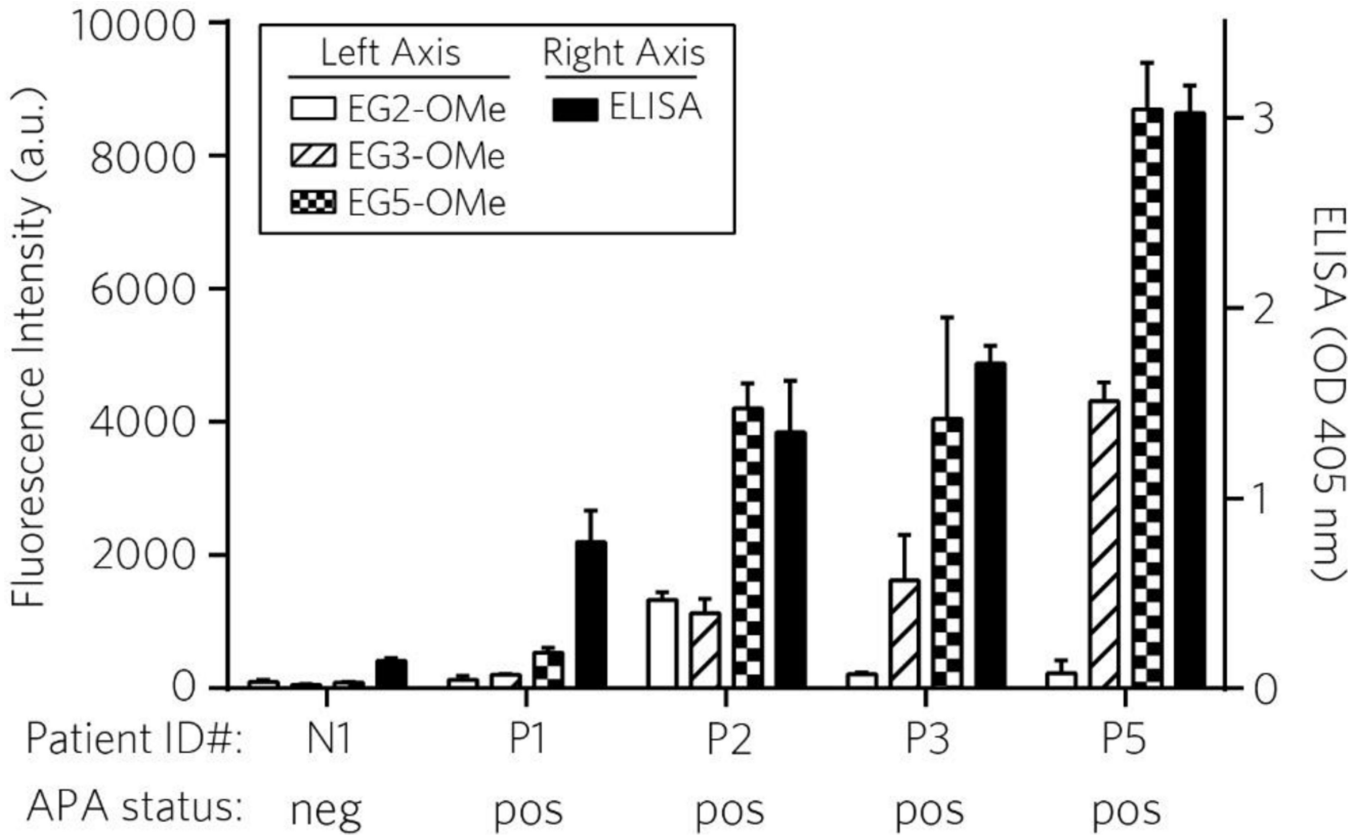

Figure 6 |. Reactivity of EG2-OMe, EG3-OMe, EG5-OMe POEGMA brushes towards APAs in patient plasma.

Four known APA-positive and one known APA-negative plasma samples were assessed by indirect ELISA against Adagen-coated plates for detecting bound IgG (right axis; solid black bars), and also by surface fluoroimmunoassay toward EG2-OMe, EG3-OMe, and EG5-OMe bottlebrush surfaces (left axis; empty, striped, and checkered bars, respectively). Results are shown as mean ± s.d. (n = 5 replicates for ELISA, n = 4 replicates for EG2-OMe and EG5-OMe, and n = 2 for EG3-OMe).

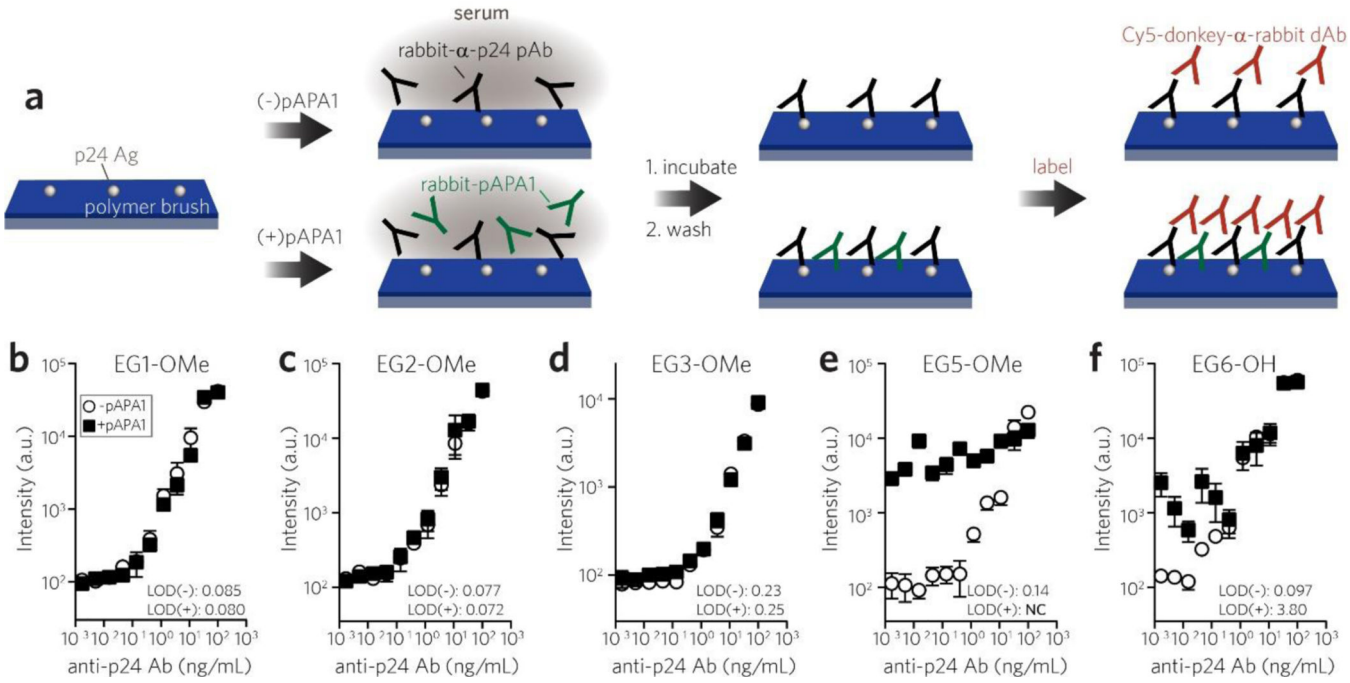

Figure 7 |.

Evaluating interference from APA reactivity in indirect sandwich immunoassays (ISIAs) for antibody detection ("serology") fabricated on polymer bottlebrushes. **a,** Schematic of serological antibody ISIA. ISIAs comprised of p24 Ag spotted onto bottlebrush overlayers were incubated with a dilution series of rabbit anti-HIV p24 polyclonal Ab, either with (bottom pathway) or without (top pathway) the presence of APA interferent (pAPA1). Surfaces were labeled with Cy5-donkey-anti-rabbit dAb, and then read by a scanner. **b, c, d, e, f,** Concentration binding curves for detecting polyclonal anti-p24 Ab (analyte) on polymer brush-based ISIAs, either with or without 100 ng/mL of APA interferent (black squares and open circles, respectively). LODs for each curve are provided in ng/mL, except for the EG5-OMe curve run with APA interferent, which was not calculated due to high background noise. Each data point represents mean ± s.d. from duplicate runs.